Weierstraß-Institut
für Angewandte Analysis und Stochastik

im Forschungsverbund Berlin e.V.

Preprint ISSN 0946 – 8633

On modeling acoustic waves in saturated poroelastic media

Bettina Albers, Krzysztof Wilmański

submitted: 2nd October 2003

Weierstrass Institute
for Applied Analysis
and Stochastics
Mohrenstraße 39
10117 Berlin
Germany
E-Mail: albers@wias-berlin.de
wilmansk@wias-berlin.de

No. 874
Berlin 2003

2000 *Mathematics Subject Classification.* 74F10, 74J05, 74L05.

Key words and phrases. Bulk waves in poroelastic materials, Biot-Gassmann model of granular materials.

Edited by
Weierstraß-Institut für Angewandte Analysis und Stochastik (WIAS)
Mohrenstraße 39
D — 10117 Berlin
Germany

Fax: + 49 30 2044975
E-Mail: preprint@wias-berlin.de
World Wide Web: http://www.wias-berlin.de/

Abstract

In the paper we present a comparison of the linear wave analysis for four models of poroelastic materials. As shown in the paper [10] a nonlinear thermodynamical construction of a two-component model of such materials requires a dependence on porosity gradient. In the linear version this dependence may or may not be present [14]. Consequently we may work with the model without a dependence on this gradient which is identical with Biot's model or we can use the so-called full model. In both cases we can construct simplified models without a coupling between partial stresses introduced by Biot. These simplified models have an adavantage that their application to, for instance, surface wave analysis yields much simpler mathematical problems.

In the present work we show that such a simplification for granular materials leads to a good qualitative agreement of all four models in ranges of porosity and Poisson's ratio commonly appearing in geotechnical applications. Quantitative differences depend on the mode of propagation and vary between 10% and 20%. We illustrate the analysis with a numerical example corresponding to data for sands.

Simultaneously we demonstrate severe limitations of applicability of Gassmann relations which yield an instability of models in a wide range of practically important values of parameters.

1 Introduction

Propagation of the so-called *second sound* was discovered in the analysis of helium II by Tisza [1] and Landau [2]. This acoustic wave describes the heat propagation in the liquid helium. Landau developed a phenomenological model which can be put into the frame of a modern phenomenological theory of mixtures [3] and which reproduces main features of this phenomenon. A review of the subject, in particular – propagation of the second sound in crystals, can be found in the work [4].

This property of many materials that they can carry more than one sound wave has been overlooked for a long time because these additional modes of propagation are very strongly attenuated. Liquid helium was an exception because experiments on this material were performed in very low temperatures in which the attenuation becomes much weaker.

Frenkel [5] proposed in 1944 a linear two-component model for elastic soils which contains all elements of the modern theory of immiscible mixtures - two kinematics, porosity as a microstructural variable, micro-macro relations among material parameters. His equations of motion (22) and (23a) remind these which we discuss in the present work except of nonsymmetric interactions between stresses. Frenkel's model – as shown by Frenkel in the same work – predicts the second sound in soils even though he claims that due to "*a very large damping ... the waves of the second kind are really non-existent*".

Independently Biot introduced in 1941 a similar model with symmetric interactions between stresses (see the collection of Biot's papers edited by Tolstoy [6]). In his works [7] he shows the existence of the second sound within his model. Since this work the prediction of the second sound in porous materials is attributed to Biot and the wave itself is carrying either the name P2-wave – in contrast to the fast longitudinal P1-wave – or Biot's wave.

Observations of P2-waves in porous materials are very difficult indeed. A series of experiments on an artificial porous material (sintered glass), in which P2-waves were observed and measured, has been performed by Plona (e.g. [8]). Measurements of P2-waves in real materials are still a subject of research (e.g. [9]).

It is worth mentioning that any hyperbolic model of a system with more than one kinematics predicts such modes. Of course, in the case of a two-component model there exists just one additional sound wave.

In this work we investigate the propagation of bulk waves within the frame of four different linear two-component models of poroelastic materials. It has been shown [10] that the Biot's model may follow from a general nonlinear thermodynamical model solely in the case when such a nonlinear model contains a constitutive dependence on the porosity gradient and, if needed, on some other higher gradients. A full linear model following from such a generalization is presented in the next section. A contribution of the porosity gradient is characterized by the material parameter N. When this parameter is zero the model is identical with this proposed by Biot provided that we neglect added mass effects. Simultaneously, it has been shown that, for a class of granular materials for which one can apply Gassmann relations between macroscopic and microscopic (true) material parameters, Biot's model as a particular case with $N = 0$ is thermodynamically admissible. Consequently we may describe a porous material ether by a model with $N \neq 0$ and corresponding generalizations of Gassmann relations or by a model with $N = 0$ (Biot) with classical Gassmann relations.

We have also two other possibilities in which the Biot's coupling between partial stresses described by the material parameter Q does not appear. Such a model has been introduced some ten years ago (e.g. see [11] where both the model and some results for waves are presented) and its structure is similar to the so-called *simple mixtures* of fluids [3]. This model follows from the Biot's model in which we substitute $Q = 0$ or from the full model with $Q = 0, N = 0$. The results are not the same because the simplified model does not admit simple tests yielding Gassmann relations. Consequently, we may use either classical Gassmann relations if we consider the simplified model to be a particular case of Biot's model or generalized Gassmann relations if we consider the simplified model to be a particular case of the full model.

Wave analysis within the simplified model is much simpler than within Biot's model or the full model. This concerns particularly surface waves which are, however, not the subject of this article. Hence it is desirable to know whether such an analysis may describe – at least qualitatively – wave properties which would follow from more general models.

We compare numerical results for the above mentioned four possibilities.

2 Linear isothermal model with porosity gradient; relation to Biot's model

A continuous linear two-component model of isothermal processes in poroelastic materials is based on the following fields

$$\left\{\rho^S, \rho^F, \mathbf{v}^S, \mathbf{e}^S, \mathbf{v}^F, n\right\} : \mathcal{B} \times \mathcal{T} \rightarrow \mathcal{V}^{15}, \tag{1}$$

defined on a domain $\mathcal{B} \subset \Re^3$ which is identified with an initial configuration of the body and on an interval of time $\mathcal{T}$. Scalars ρ^S, ρ^F are the partial mass densities of the skeleton, and of the fluid component, respectively, and they are related to true mass densities ρ^{SR}, ρ^{FR} in the following way

$$\rho^S = (1-n)\,\rho^{SR}, \quad \rho^F = n\rho^{FR}, \tag{2}$$

where n is the current porosity (volume fraction of voids in the skeleton).

Vectors $\mathbf{v}^S, \mathbf{v}^F$ describe macroscopic partial velocities of the skeleton, and of the fluid, respectively. In many cases the difference $\mathbf{v}^F - \mathbf{v}^S$ can be approximately identified with the so-called filter velocity (diffusion velocity).

The symmetric tensor $\mathbf{e}^S$ describes macroscopic deformations of the skeleton. For small deformations (a linear model!) it satisfies the following kinematic compatibility relation

$$\frac{\partial \mathbf{e}^S}{\partial t} = \text{sym grad}\,\mathbf{v}^S \equiv \frac{1}{2}\left[\text{grad}\,\mathbf{v}^S + \left(\text{grad}\,\mathbf{v}^S\right)^T\right]. \tag{3}$$

The model which describes the behavior of these fields follows from the set of balance equations (again linear!)

$$\begin{aligned}
\frac{\partial \rho^S}{\partial t} &= -\rho_0^S \operatorname{div}\mathbf{v}^S, \quad \frac{\partial \rho^F}{\partial t} = -\rho_0^F \operatorname{div}\mathbf{v}^F, \\
\rho_0^S \frac{\partial \mathbf{v}^S}{\partial t} &= \operatorname{div}\mathbf{T}^S + \hat{\mathbf{p}} + \rho_0^S \mathbf{b}^S, \\
\rho_0^F \frac{\partial \mathbf{v}^F}{\partial t} &= \operatorname{div}\mathbf{T}^F - \hat{\mathbf{p}} + \rho_0^F \mathbf{b}^F,
\end{aligned} \tag{4}$$

$$\frac{\partial\left(n-n_E\right)}{\partial t} = -\Phi \operatorname{div}\left(\mathbf{v}^F - \mathbf{v}^S\right) + \hat{n}. \tag{5}$$

The index 0 refers always to a reference value of a quantity.

In these equations the symmetric tensors $\mathbf{T}^S, \mathbf{T}^F$ are partial Cauchy stresses, $\hat{\mathbf{p}}$ is the momentum source, $\mathbf{b}^S, \mathbf{b}^F$ are partial body forces, n_E is the so-called equilibrium porosity, Φ is the transport coefficient of porosity, and $\hat{n}$ is the porosity source. Further we neglect the last contribution and this means that we do not account for processes of spontaneous relaxation of porosity.

These balance equations transform into field equations for fields (1) if we add constitutive relations. For poroelastic materials they are assumed to have the form

$$\begin{aligned}
\mathbf{T}^S &= \mathbf{T}_0^S + \lambda^S e\mathbf{1} + 2\mu^S \mathbf{e}^S + Q\varepsilon\mathbf{1}, \quad e := \operatorname{tr}\mathbf{e}^S, \quad \varepsilon := \frac{\rho_0^F - \rho^F}{\rho_0^F}, \\
\mathbf{T}^F &= \mathbf{T}_0^F + \rho_0^F \kappa\varepsilon\mathbf{1} + Qe\mathbf{1}, \quad n_E = n_0\left(1 + \delta e\right), \\
\hat{\mathbf{p}} &= \pi\left(\mathbf{v}^F - \mathbf{v}^S\right) - N \operatorname{grad} n.
\end{aligned} \tag{6}$$

Certainly, the effective (macroscopic) parameters λ^S, μ^S correspond to classical Lamé constants, κ describes the macroscopic compressibility of the fluid, δ is a parameter coupling equilibrium changes of porosity with volume changes of the skeleton, e, Q is the coupling parameter introduced by Biot, and N is a parameter describing the influence of the porosity gradient. The permeability coefficient π is related to the permeability appearing in the Darcy model of seepage.

The above material parameters can be transformed into the classical Biot's parameters (e.g. [12]) by the following formulae

$$K := \lambda^S + \frac{2}{3}\mu^S + \rho_0^F\kappa + 2Q, \quad C := \frac{1}{n_0}\left(Q + \rho_0^F\kappa\right), \quad M := \frac{\rho_0^F\kappa}{n_0^2}. \tag{7}$$

Partial mass balance equations can be easily written in the following form

$$\frac{\partial e}{\partial t} = \operatorname{div}\mathbf{v}^S, \quad \frac{\partial \varepsilon}{\partial t} = \operatorname{div}\mathbf{v}^F, \quad e = \frac{\rho_0^S - \rho^S}{\rho_0^S}, \tag{8}$$

and the porosity balance equation with $\hat{n} \equiv 0$ yields the following relation for changes of porosity:

$$n = n_0\left[1 + \delta e + \frac{\Phi}{n_0}\left(e - \varepsilon\right)\right]. \tag{9}$$

This relation for porosity changes yields explicit corrections of constitutive relations for partial stresses provided the initial porosity n_0 is constant. Then we can incorporate the contribution $N \operatorname{grad} n$ of the momentum source into these relations in the following way

$$\begin{aligned}
\mathbf{T}^S &= \mathbf{T}_0^S + \lambda^S e\mathbf{1} + 2\mu^S \mathbf{e}^S + Q\varepsilon\mathbf{1} - N(n - n_0)\mathbf{1}, \\
\mathbf{T}^F &= \mathbf{T}_0^F + \rho_0^F\kappa\varepsilon\mathbf{1} + Qe\mathbf{1} + N(n - n_0)\mathbf{1}, \\
\hat{\mathbf{p}} &= \pi\left(\mathbf{v}^F - \mathbf{v}^S\right), \quad n - n_0 = n_0\delta e + \Phi\left(e - \varepsilon\right).
\end{aligned} \tag{10}$$

This is the form of constitutive relations which we use further in this work.

3 Material parameters for granular materials – Gassmann relations

The above phenomenological model does not specify the way in which material parameters depend on porosity. For many materials, such as rocks or biological tissues, this dependence must be found experimentally. However, for granular materials Gassmann proposed a procedure relating some macroscopic parameters to microscopic compressibilities of solid and fluid phases and to the porosity. If we use Biot's material parameters these relations concern K, M, C and they have the form (e.g. [12])

$$
\begin{aligned}
&K = K_d + \frac{(K_s - K_d)^2}{\frac{K_s^2}{K_W} - K_d} + K_d, \quad C = \frac{K_s(K_s - K_d)}{\frac{K_s^2}{K_W} - K_d}, \quad M = \frac{K_s^2}{\frac{K_s^2}{K_W} - K_d}, \qquad (11)\\
&\frac{1}{K_W} := \frac{1-n_0}{K_s} + \frac{n_0}{K_f},
\end{aligned}
$$

where K_s, K_f are compressibility modulae of the grains, and of the true fluid, respectively, and K_d is the so-called drained compressibility modulus and it is assumed to be known. It can be either measured on drained samples or it can be given by a heuristic formula. Such a formula has been proposed, for example, by Geertsma [13]

$$
K_d = \frac{K_s}{1 + g n_0}, \qquad (12)
$$

where g is an empirical parameter. As claimed by White [13] the value $g = 50$ corresponds well with experimental data for many soils.

The above relations for K, C, M can be derived systematically by means of a micro-macro transition procedure [14]. This procedure yields the following equations

$$
\begin{aligned}
0 &= C + \frac{K_f(K - K_s) - N(K - K_V)}{n_0(K_s - K_f)},\\
0 &= n_0 - \frac{C}{M} - \frac{K_b}{K_s}\frac{1 - (1-n_0)\frac{K_s}{K_b}}{1 - \frac{1-n_0}{n_0}\frac{NC}{K_b M}}\left[1 - \frac{N(K - n_0 C)}{n_0 M K_b}\right],\\
0 &= K - K_d - C\frac{C - N}{M - \frac{N}{n_0}}, \qquad (13)\\
0 &= \left(1 - \frac{K}{K_W}\right)\left(M - C - N\frac{1-n_0}{n_0}\frac{C}{K_s}\right) +\\
&\quad + \left(1 - \frac{C}{K_W}\right)\left(K - C - N\frac{1-n_0}{n_0}\left(1 - \frac{K}{K_s}\right)\right),
\end{aligned}
$$

where

$$
K_b := K - \frac{C^2}{M}. \qquad (14)
$$

It is easy to check that Gassmann relations (11) satisfy equations (13) with $N \equiv 0$. Otherwise we can solve the above equations numerically and find relations

$$\begin{aligned} K &= K\left(n_0, K_s, K_f\right), \quad C = C\left(n_0, K_s, K_f\right), \\ M &= M\left(n_0, K_s, K_f\right), \quad N = N\left(n_0, K_s, K_f\right). \end{aligned} \tag{15}$$

Then by means of (7) we can find $\left\{\lambda^S + \frac{2}{3}\mu^S, \kappa, Q\right\}$.

In addition we obtain the following relations for parameters specifying changes of porosity

$$\begin{aligned} \delta &= \frac{K_V - K}{n_0\left(K_s - K_f\right)}, \quad \Phi = \frac{\rho_0^F \kappa + Q - n_0 K_f}{K_s - K_f}, \\ K_V &:= (1 - n_0)K_s + n_0 K_f. \end{aligned} \tag{16}$$

There remain material parameters π, μ^S whose dependence on n_0 cannot be specified by means of the above mentioned procedure. For the purpose of this work we make the assumption that π is related to the hydraulic conductivity K, appearing in Darcy's law, by the following formula

$$\pi = n_0 \frac{\rho_0^{FR} g_{earth}}{\mathrm{K}}, \tag{17}$$

where ρ_0^{FR} is the true initial mass density of the fluid and g_{earth} is the earth acceleration. This formula follows as an approximation from the momentum balance equation for the fluid $(4)_4$. Namely, if we neglect the acceleration and body forces and substitute $\mathbf{T}^F = -n_0 p_f \mathbf{1}$, where p_f is the pore pressure then $\operatorname{grad} p_f = -\frac{\pi}{n_0}\left(\mathbf{v}^F - \mathbf{v}^S\right)$, and the comparison with the Darcy's law yields $\frac{\pi}{n_0} = \rho_0^{FR} g_{earth}/\mathrm{K}$. This may be not a bad approximation for intermediate values of porosity, say, for n_0 between 0.2 and 0.5. In general, one would have to rely on some empirical relation.

For the shear modulus we can at least introduce a relation to the Poisson's ratio ν. It is convenient because there are indications that the dependence of Poisson's ratio on porosity is weak – again at least for intermediate porosities. We proceed to present this relation.

The basis for the derivation is the assumption that in drained experiments the two-component poroelastic material satisfies classical relations for the full stresses in the elastic one-component material. In such experiments $\mathbf{T}^F - \mathbf{T}_0^F = 0$. Then relations (10) yield after easy manipulations (see: Appendix)

$$\mu^S = \frac{3}{2}\frac{1-2\nu}{1+\nu}\left\{K_d + Q\frac{Q + n_0 N}{\rho_0^F \kappa - n_0 N} - \frac{Q^2 + N\left[\rho_0^F \kappa\left(n_0\delta + \Phi\right) + Q\left(n_0\delta + 2\Phi\right)\right]}{\rho_0^F \kappa - \Phi N}\right\}. \tag{18}$$

Clearly, for $N = 0$ this relation becomes

$$\mu^S = \frac{3}{2}\frac{1-2\nu}{1+\nu}\frac{K_s}{1 + g n_0}. \tag{19}$$

Consequently, the effective shear modulus is independent of the coupling between components described by the parameter Q.

This is not true in the general case when $N \neq 0$. Moreover, if we apply micro-macro relations following from (13) the contribution with the minus sign may dominate in this formula. This yields a negative value of the shear modulus μ^S and, consequently, a structural instability of the model forbidden by the thermodynamical condition of concave entropy. We demonstrate this property caused by the Gassmann relations on a numerical example presented further in this work.

4 Propagation of fronts of weak discontinuity waves

We begin the analysis of propagation of weak discontinuity waves by the investigation of the front. The front of such a wave is defined as a smooth moving surface on which the fields are continuous but their derivatives may have finite discontinuities

$$\begin{gathered}\left[\left[\mathbf{v}^S\right]\right]=0, \quad \left[\left[\mathbf{v}^F\right]\right]=0, \quad \left[\left[\mathbf{e}^S\right]\right]=0, \quad [[\varepsilon]]=0, \\ \mathbf{a}^S:=\left[\left[\frac{\partial \mathbf{v}^S}{\partial t}\right]\right]\neq 0, \quad \mathbf{a}^F:=\left[\left[\frac{\partial \mathbf{v}^F}{\partial t}\right]\right]\neq 0,\end{gathered} \tag{20}$$

where the double bracket denotes the jump through the surface $[[\cdots]]:=(\cdots)^+-(\cdots)^-$, the quantities on the right hand side are limits of the quantities on the positive and negative side of the surface, respectively.

The fields satisfying the above conditions must fulfil the kinematic compatibility conditions on the front which follow from general so-called Maxwell conditions. They have the form

$$\begin{aligned}\left[\left[\operatorname{grad}\mathbf{v}^S\right]\right] &= -\frac{1}{c}\mathbf{a}^S\otimes\mathbf{n}, \quad \left[\left[\operatorname{grad}\mathbf{v}^F\right]\right]=-\frac{1}{c}\mathbf{a}^F\otimes\mathbf{n}, \\ \left[\left[\operatorname{grad}\mathbf{e}^S\right]\right] &= -\frac{1}{c}\left[\left[\frac{\partial \mathbf{e}^S}{\partial t}\right]\right]\otimes\mathbf{n}, \quad [[\operatorname{grad}\varepsilon]]=-\frac{1}{c}\left[\left[\frac{\partial \varepsilon}{\partial t}\right]\right]\mathbf{n},\end{aligned} \tag{21}$$

where c is the *velocity of propagation* of the front and $\mathbf{n}$ is the unit vector perpendicular to the front.

Bearing relations (3), $(8)_2$ in mind we obtain immediately

$$\begin{aligned}\left[\left[\frac{\partial \mathbf{e}^S}{\partial t}\right]\right] &= -\frac{1}{2c}\left(\mathbf{a}^S\otimes\mathbf{n}+\mathbf{n}\otimes\mathbf{a}^S\right), \quad \left[\left[\operatorname{grad}\mathbf{e}^S\right]\right]=\frac{1}{2c^2}\left(\mathbf{a}^S\otimes\mathbf{n}+\mathbf{n}\otimes\mathbf{a}^S\right)\otimes\mathbf{n}, \\ \left[\left[\frac{\partial \varepsilon}{\partial t}\right]\right] &= -\frac{1}{c}\mathbf{a}^F\cdot\mathbf{n}, \quad [[\operatorname{grad}\varepsilon]]=\frac{1}{c^2}\mathbf{a}^F\cdot\mathbf{n}\mathbf{n}.\end{aligned} \tag{22}$$

Now we form the jump of field equations on the front. After easy calculations it follows from (4) and (10)

$$\left\{\rho_0^S c^2\mathbf{1}-\lambda^S\mathbf{n}\otimes\mathbf{n}-\mu^S\left(\mathbf{1}+\mathbf{n}\otimes\mathbf{n}\right)+N\left(n_0\delta+\Phi\right)\mathbf{n}\otimes\mathbf{n}\right\}\mathbf{a}^S-$$

$$-\left\{Q\mathbf{n}\otimes\mathbf{n}+N\Phi\mathbf{n}\otimes\mathbf{n}\right\}\mathbf{a}^F=0, \tag{23}$$

$$-\left\{Q\mathbf{n}\otimes\mathbf{n}+N\left(n_0\delta+\Phi\right)\mathbf{n}\otimes\mathbf{n}\right\}\mathbf{a}^S+\left\{\rho_0^F c^2\mathbf{1}-\rho_0^F\kappa\mathbf{n}\otimes\mathbf{n}+N\Phi\mathbf{n}\otimes\mathbf{n}\right\}\mathbf{a}^F=0. \tag{24}$$

This is an eigenvalue problem. We split it into the normal part parallel to $\mathbf{n}$ and the transversal part perpendicular to $\mathbf{n}$.

In the first case we obtain

$$\begin{aligned}\left\{\rho_0^S c^2-\left(\lambda^S+2\mu^S\right)+N\left(n_0\delta+\Phi\right)\right\}a_n^S-\left\{Q+N\Phi\right\}a_n^F &= 0, \\ -\left\{Q+N\left(n_0\delta+\Phi\right)\right\}a_n^S+\left\{\rho_0^F c^2-\rho_0^F\kappa+N\Phi\right\}a_n^F &= 0,\end{aligned} \tag{25}$$

$$a_n^S:=\mathbf{a}^S\cdot\mathbf{n},\quad a_n^F:=\mathbf{a}^F\cdot\mathbf{n},$$

This homogeneous set of equations possesses a nontrivial solution if the determinant vanishes. We obtain the following *propagation condition*

$$c^4-c^2\left\{\frac{\lambda^S+2\mu^S-N\left(n_0\delta+\Phi\right)}{\rho_0^S}+\frac{\rho_0^F\kappa-N\Phi}{\rho_0^F}\right\}+$$

$$+\left\{\frac{\left(\lambda^S+2\mu^S\right)-N\left(n_0\delta+\Phi\right)}{\rho_0^S}\right\}\left\{\frac{\rho_0^F\kappa-N\Phi}{\rho_0^F}\right\}-$$

$$-\frac{1}{\rho_0^S\rho_0^F}\left\{Q+N\Phi\right\}\left\{Q+N\left(n_0\delta+\Phi\right)\right\}=0. \tag{26}$$

This biquadratic equation for c has two positive and two negative solutions which define two *longitudinal waves*: P1-wave and P2-wave (Biot's wave). Namely

$$c^2=\frac{1}{2}\left\{\frac{\lambda^S+2\mu^S-N\left(n_0\delta+\Phi\right)}{\rho_0^S}+\frac{\rho_0^F\kappa-N\Phi}{\rho_0^F}\pm\sqrt{\Delta}\right\}, \tag{27}$$

$$\Delta:=\left\{\frac{\lambda^S+2\mu^S-N\left(n_0\delta+\Phi\right)}{\rho_0^S}-\frac{\rho_0^F\kappa-N\Phi}{\rho_0^F}\right\}^2+4\frac{\left\{Q+N\Phi\right\}\left\{Q+N\left(n_0\delta+\Phi\right)\right\}}{\rho_0^S\rho_0^F}.$$

In the second case we multiply equations (23), (24) by a unit vector $\mathbf{n}_\perp$ perpendicular to $\mathbf{n}$. We obtain

$$\left\{\rho_0^S c^2-\mu^S\right\}a_\perp^S=0,\quad a_\perp^F=0, \tag{28}$$

$$a_\perp^S:=\mathbf{a}^S\cdot\mathbf{n}_\perp,\quad a_\perp^F:=\mathbf{a}^F\cdot\mathbf{n}_\perp.$$

Hence

$$c=\sqrt{\frac{\mu^S}{\rho_0^S}}. \tag{29}$$

This is the velocity of propagation of the *transversal wave*. It looks like the corresponding formula in the classical elasticity. However couplings may have an influence on the behavior of this wave in some models which we present further in this section.

Let us mention that all these modes are attenuated due to the diffusion. This property cannot be demonstrated by means of such simple arguments for the jumps on the front. We return to the detailed calculation of attenuation in the next section.

Instead of a simple but cumbersome analytical investigation of the above solutions we present a numerical example. For this analysis we choose the following numerical data typical for sand and water

$$\begin{aligned} \rho_0^{SR} &= 2500\,\frac{kg}{m^3}, \quad \rho_0^{FR} = 1000\,\frac{kg}{m^3}, \\ K_s &= 48\,GPa, \quad K_f = 2.25\,GPa, \quad \pi = n_0 \times 10^7\,\frac{kg}{m^3 s}, \end{aligned} \tag{30}$$

which we use in the evaluation of macroscopic material parameters. The value of the permeability coefficient π corresponds to the hydraulic conductivity K= $10^{-3}\,\frac{m}{s} = 0.1\,darcy$. We present the results in dependence on varying porosity n_0 and varying Poisson's ratio ν.

In Figure 1 we show the behavior of velocities of propagation of fronts of P1-, S-, and P2-waves. These three-dimensional plots illustrate the general qualitative character of the dependence on the initial porosity n_0 and on the Poisson's ratio ν. Quantitative relations of different models shall be demonstrated further for monochromatic waves.

In order to show whole surfaces in these 3D-pictures we collected the points in bars in the direction of the ν-axis. Separation of these bars reflects the steps of numerical evaluation – for n_0 this is 0.02, and for ν – 0.01.

First of all let us point out certain general features of these plots. They were calculated by means of the relation (27), either with Gassmann relations (11) (for Biot's and "simple mixture" models) or with material parameters following from (13) (for the full models). In both cases we have used (18) for the dependence of the shear modulus μ^S on the Poisson's ratio ν.

Values of porosity vary between 0.1 and 0.58. This range has been chosen due to the applicability of the full model. Micro-macro relations for this model yield instabilities below $n_0 = 0.1$ and above the value $n_0 \approx 0.58$. Instabilities in the first region, for $n_0 < 0.1$, follow from negative values of the shear modulus for $N \neq 0$ in this range which has been indicated before. On the other hand for values of n_0 bigger than 0.58 the relations (13) yield negative values of compressibilities which do not have any physical bearing and, similarly to the first region, indicate a restriction on applicability of Gassmann relations.

Values of Poisson's ratio ν begin with 0.1. Even in the vicinity of this point and particularly below this value, as we see further, there appear instabilities which make the model not admissible. We do not attempt in this work to make improvements beyond those limits.

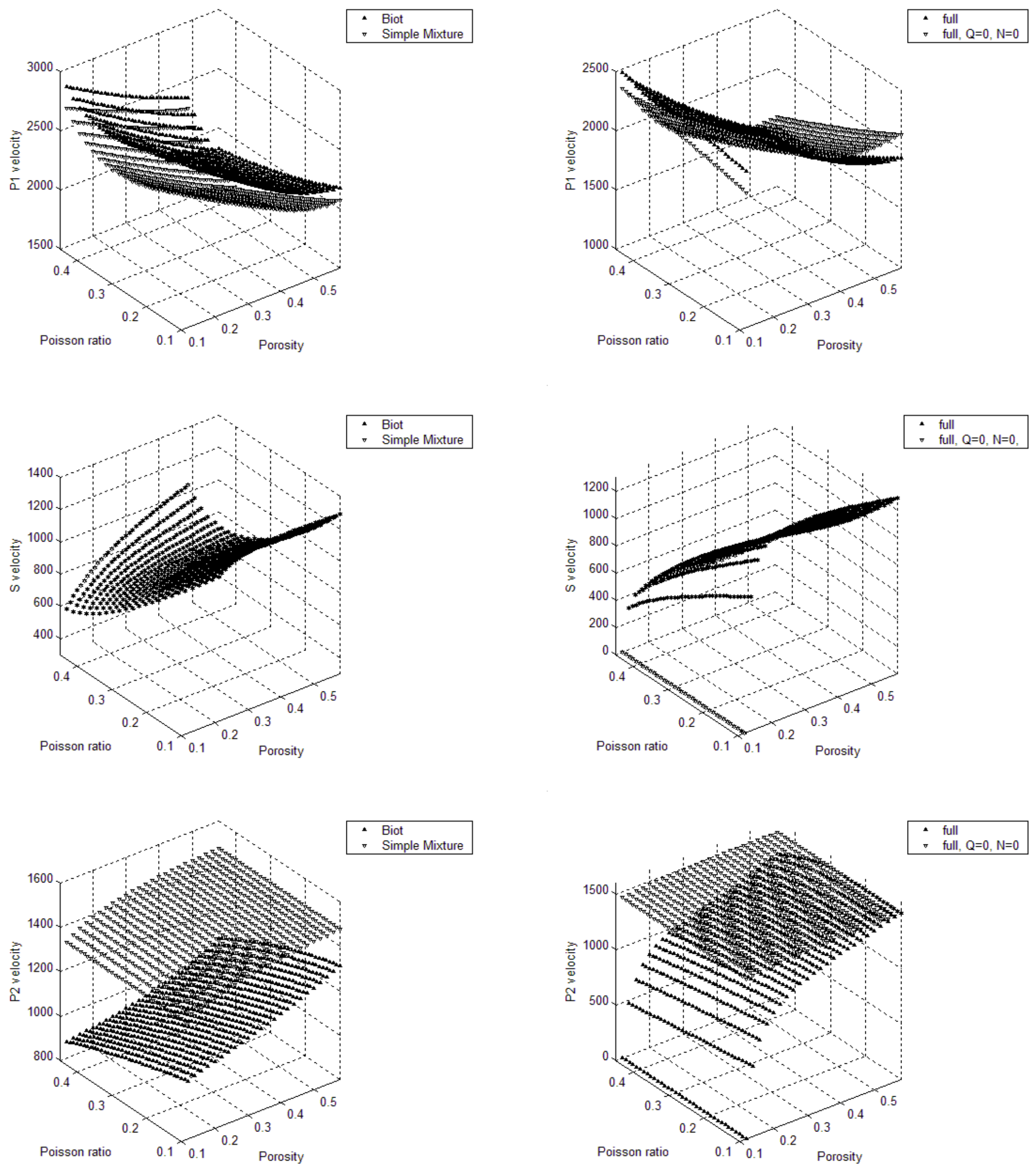

Figure 1: *Front velocities of P1-, S-, and P2-waves*

Left-hand side: Biot's model and "simple mixture" model

Right-hand Side: The full model and the simplified full model

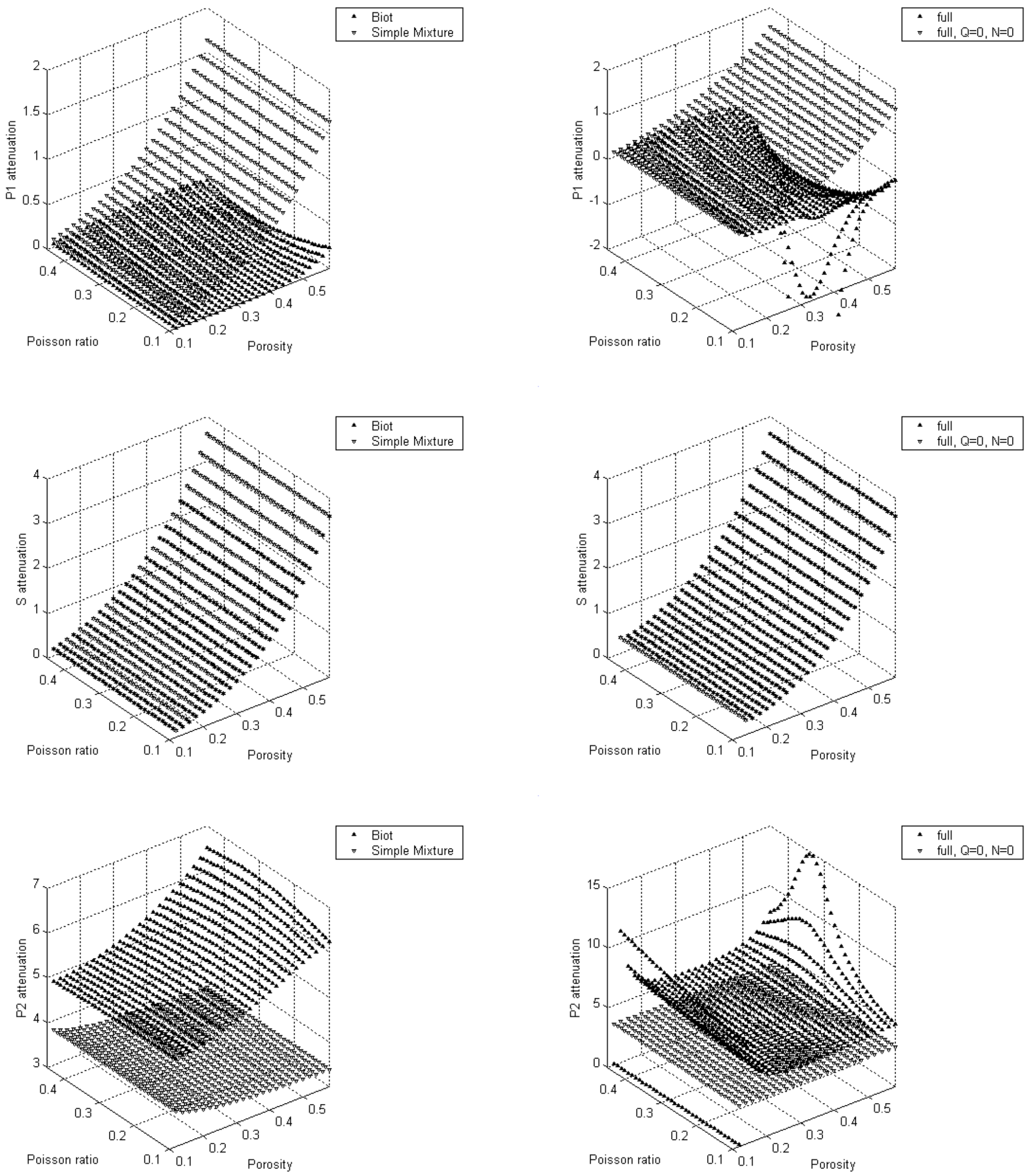

Figure 2: *Attenuation of fronts of P1-, S-, and P2-waves*

Left-hand side: Biot's model and "simple mixture" model

Right-hand Side: The full model and the simplified full model

Clearly, all above restrictions of the full model are related to the extension of Gassmann relations and, consequently, to the applicability of the full model to a certain limited class of granular materials for which we can claim Gassmann relations to hold. They may not apply to modeling of rocks, concrete and similar materials with a compact skeleton.

Plots in the left column follow for Biot's model and for its simplification which we call "simple mixture" ($Q = 0, N = 0$). For the latter model all material parameters except Q are identical with those of Biot's model. As we see the velocity of propagation of the front of P1-waves has a similar shape for both models but it is lower for the simple mixture model than for Biot's model. The difference is app. 10%. It is the opposite for P2-waves where fronts propagate faster for the simple mixture model than for Biot's model and the difference is app. 20%. Certainly, velocities of P2-waves decay to zero in both models as n_0 approaches zero.

The plot for velocities of S-waves is identical for both models.

These plots indicate already the main conclusion of the work that the qualitative behavior of Biot's model and the simple mixture model is the same and quantitative differences are small enough to be accepted in practical applications. We return to the latter point in the next two sections.

Plots for the full model and its simplification with the same values of material parameters except of $Q = 0$ and $N = 0$ are shown in the right column. For medium values of porosities and Poisson's ratio the behavior of these models is similar to Biot's model and the simple mixture model. Large deviations appear for P1-waves for small values of porosity where a dependence on the Poisson's ratio is different from Biot's model. Also for P2-waves substantial qualitative differences appear for small values of porosity and small values of the Poisson's ratio. In particular, below $n_0 \approx 0.14$ the velocity of the P2-wave within the full model decays more rapidly than within other models.

Again the velocity of the S-wave is almost identical for both models but it behaves differently from the Biot's model and simple mixture model for small porosities where it is decaying rather than growing and it possesses inflection points at app. $n_0 \approx 0.25$.

All these qualitative differences of both full models may be attributed to the singular behavior of the shear modulus μ^S. They would not appear if values of the parameter N were smaller than these predicted by Gassmann relations.

The attenuation of waves cannot be discussed by means of the simple analysis of propagation of fronts. We present analytical results for this problem in the next section (relations (38) for transversal waves and (42) for longitudinal waves). However, for completeness we already show in Figure 2 the numerical results following from the evaluation of these relations.

In spite of qualitative similarity in the whole range of parameters, quantitative differences between attenuations calculated for different models are much larger than the differences between velocities. For instance, the attenuation of the P1-wave as given by Biot's model is a few times smaller than in the simple mixture model (the left column, the upper picture). It is the other way around for P2-waves which are much stronger attenuated according to Biot's model than to the simple mixture model. However, these differences become much smaller for medium values of parameters. We discuss these differences in details for monochromatic waves.

Again the attenuation of transversal waves is the same for both models – Biot's model and the simple mixture model.

For the full model the attenuation of P1-waves becomes negative in the case of large porosities and small Poisson's ratio. The range of instability is approximately limited by the line: $n_0 = \nu$.

The attenuation of P2-waves becomes also much bigger than in Biot's model for small values of porosity.

We return in the next section to the explanation of the above indicated instabilities.

In contrast to a singular behavior near the limits of n_0 and ν results seem to agree well in practically relevant medium values of porosity and of Poisson's ratio.

5 Monochromatic bulk waves

We proceed to investigate the propagation conditions for monochromatic waves. These waves are solutions in the infinite domain based on the following ansatz

$$\begin{aligned} &\mathbf{v}^S = \mathbf{V}^S \mathcal{E}, \quad \mathbf{v}^F = \mathbf{V}^F \mathcal{E}, \quad ,\mathbf{e}^S = \mathbf{E}^S \mathcal{E}, \quad \varepsilon = E^F \mathcal{E}, \\ &\mathcal{E} := \exp\left[i\left(k\mathbf{n}\cdot\mathbf{x} - \omega t\right)\right], \end{aligned} \tag{31}$$

where $\mathbf{V}^S, \mathbf{V}^F, \mathbf{E}^S, E^F$ are constant *amplitudes*, ω is a given real *frequency*, k is a complex *wave number*, and $\mathbf{n}$ is a unit vector pointing in the direction of propagation of the wave.

Substitution of (31) in relations (3), $(8)_2$ yields the following auxiliary relations

$$\mathbf{E}^S = -\frac{k}{2\omega}(\mathbf{n}\otimes\mathbf{V}^S + \mathbf{V}^S\otimes\mathbf{n}), \quad E^F = -\frac{k}{\omega}\mathbf{V}^F\cdot\mathbf{n}. \tag{32}$$

Consequently, by means of momentum balance equations we obtain the following set of equations for amplitudes $\mathbf{V}^S, \mathbf{V}^F$

$$\begin{aligned} &\left[\rho_0^S\omega^2\mathbf{1} - \lambda^S k^2\mathbf{n}\otimes\mathbf{n} - \mu^S k^2(\mathbf{n}\otimes\mathbf{n} + \mathbf{1}) + N\left(n_0\delta + \Phi\right)k^2\mathbf{n}\otimes\mathbf{n} + i\pi\omega\mathbf{1}\right]\mathbf{V}^S - \\ &\quad - \left[Qk^2\mathbf{n}\otimes\mathbf{n} + N\Phi k^2\mathbf{n}\otimes\mathbf{n} + i\pi\omega\mathbf{1}\right]\mathbf{V}^F = 0, \end{aligned} \tag{33}$$

$$\begin{aligned} &-\left[Qk^2\mathbf{n}\otimes\mathbf{n} + N\left(n_0\delta + \Phi\right)k^2\mathbf{n}\otimes\mathbf{n} + i\pi\omega\mathbf{1}\right]\mathbf{V}^S + \\ &+\left[\rho_0^F\omega^2\mathbf{1} - \rho_0^F\kappa k^2\mathbf{n}\otimes\mathbf{n} + N\Phi k^2\mathbf{n}\otimes\mathbf{n} + i\pi\omega\mathbf{1}\right]\mathbf{V}^F = 0. \end{aligned} \tag{34}$$

This is again an eigenvalue problem. It looks similar to (23), (24) except of contributions with the permeability π. As before we separate the component perpendicular to $\mathbf{n}$ (transversal waves) and the component parallel to $\mathbf{n}$ (longitudinal waves).

– Transversal waves.

Let us multiply equations (33), (34) by a unit vector $\mathbf{n}_\perp$ perpendicular to $\mathbf{n}$. Then we obtain

$$\begin{aligned}\left(\rho_0^S\omega^2 - \mu^S k^2 + i\pi\omega\right) V_\perp^S - i\pi\omega V_\perp^F &= 0, \\ -i\pi\omega V_\perp^S + \left(\rho_0^F\omega^2 - \mu^S k^2\right) V_\perp^F &= 0.\end{aligned} \tag{35}$$

$$V_\perp^S := \mathbf{V}^S \cdot \mathbf{n}_\perp, \quad V_\perp^F := \mathbf{V}^F \cdot \mathbf{n}_\perp,$$

The condition that the determinant of this set must vanish yields the following *dispersion relation*

$$\left(\omega^2 - \frac{\mu^S}{\rho_0^S}k^2\right) + i\pi\frac{1}{\omega}\frac{\rho_0^S + \rho_0^F}{\rho_0^S\rho_0^F}\left(\omega^2 - \frac{\mu^S}{\rho_0^S + \rho_0^F}k^2\right) = 0. \tag{36}$$

Solutions of this equation $k = k(\omega)$ specify both the phase velocity of transversal waves $c_{ph} = \frac{\omega}{\mathrm{Re}\,(k)}$ and the attenuation $\mathrm{Im}\,(k)$. We present a numerical example of these solutions further in this work. However, some important properties of equation (36) should be mentioned. First of all, this equation does not contain the parameter Q which means that transversal (shear) waves are identical for the three models considered in this work in which $N = 0$. Then the relation (19) for μ^S holds true. Secondly, the velocity of propagation in the limit $\omega \to \infty$ is identical with this of the front (29) and different from the other important limit $\omega \to 0$. We have

$$\lim_{\omega\to\infty} c_{ph} = \sqrt{\frac{\mu^S}{\rho_0^S}}, \quad \lim_{\omega\to 0} c_{ph} = \sqrt{\frac{\mu^S}{\rho_0^S + \rho_0^F}}. \tag{37}$$

Finally the attenuation for these two limits follows also easily from (36) and we have

$$\lim_{\omega\to\infty} \mathrm{Im}\,(k) = \frac{\pi}{2\rho_0^S\sqrt{\frac{\mu^S}{\rho_0^S}}}, \quad \lim_{\omega\to 0} \mathrm{Im}\,(k) = 0. \tag{38}$$

– Longitudinal waves.

Now we multiply equations (33), (34) by the vector $\mathbf{n}$. It follows

$$\begin{gathered}\left\{\rho_0^S\omega^2 - \left[\lambda^S + 2\mu^S - N\left(n_0\delta + \Phi\right)\right]k^2 + i\pi\omega\right\} V_n^S - \left\{\left[Q + N\Phi\right]k^2 + i\pi\omega\right\} V_n^F = 0, \\ -\left\{\left[Q + N\left(n_0\delta + \Phi\right)\right]k^2 + i\pi\omega\right\} V_n^S + \left\{\rho_0^F\omega^2 - \left[\rho_0^F\kappa - N\Phi\right]k^2 + i\pi\omega\right\} V_n^F = 0, \\ V_n^S := \mathbf{V}^S \cdot \mathbf{n}, \quad V_n^F := \mathbf{V}^F \cdot \mathbf{n},\end{gathered} \tag{39}$$

Consequently, we obtain the following dispersion relation for these waves

$$k^4\left\{\left[\lambda^S + 2\mu^S - N\left(n_0\delta + \Phi\right)\right]\left[\rho_0^F\kappa - N\Phi\right] - \left[Q + N\left(n_0\delta + \Phi\right)\right]\left[Q + N\Phi\right]\right\} -$$

$$-k^2\left\{\left(\rho_0^S\omega^2+i\pi\omega\right)\left[\rho_0^F\kappa-N\Phi\right]+\left(\rho_0^F\omega^2+i\pi\omega\right)\left[\lambda^S+2\mu^S-N\left(n_0\delta+\Phi\right)\right]+\right.$$
$$\left.+i\pi\omega\left[2Q+N\left(n_0\delta+\Phi\right)\right]\right\}+ \tag{40}$$
$$+\left(\rho_0^S\omega^2+i\pi\omega\right)\left(\rho_0^F\omega^2+i\pi\omega\right)+\pi^2\omega^2=0.$$

Before we proceed to demonstrate properties of $k(\omega)$ on numerical examples let us discuss some features of the above relation for the limit values of frequencies.

For $\omega\to\infty$ we obtain the following relations

$$c^4-c^2\left\{c_{P1}^2+c_{P2}^2-\frac{N}{\rho_0^S}\left[n_0\delta+\left(1+\frac{1}{r}\right)\Phi\right]\right\}+$$
$$+\left\{c_{P1}^2c_{P2}^2-\frac{Q^2}{r\rho_0^{S2}}-\frac{N}{r\rho_0^S}\left[c_{P1}^2\Phi+rc_{P2}^2\left(n_0\delta+\Phi\right)+\frac{Q}{\rho_0^S}\left(n_0\delta+2\Phi\right)\right]\right\}=0, \tag{41}$$

$$\operatorname{Im}(k)=-(-1)^\alpha\frac{\pi}{2\rho_0^S c_\alpha}\frac{\frac{1}{r}\left(c_{P1}^2-c_\alpha^2\right)+\left(c_{P2}^2-c_\alpha^2\right)+\frac{2Q}{r\rho_0^S}-\frac{1}{r}\frac{N}{\rho_0^S}\Phi}{c_2^2-c_1^2},\qquad \alpha=1,2, \tag{42}$$

where

$$c:=\lim_{\omega\to\infty}\frac{\omega}{\operatorname{Re}(k)},\qquad c_{P1}^2:=\frac{\lambda^S+2\mu^S}{\rho_0^S},\qquad c_{P2}^2:=\kappa, \tag{43}$$

and $c_\alpha,\alpha=1,2$ are two positive solutions of the equation (41).

Obviously, after trivial reshuffling of terms equation (41) coincides with equation (26). This means that the velocities of wave fronts are identical with the phase velocities of monochromatic waves in the limit $\omega\to\infty$.

Simultaneously, relation (42) specifies the attenuation of fronts which could not be calculated by means of the analysis of singularities presented in the previous section. Numerical results for this relation have been presented in Figure 2.

As we discuss further in some details an important difference between Biot's model and the simple mixture model in relation to the limits $\omega\to 0$ and $\omega\to\infty$ we quote these results in the explicit form. We have the following phase velocities and attenuations within Biot's model

– low frequency limit $\omega\to 0$

$$\lim_{\omega\to 0}\left(\frac{\omega}{k_R}\right)^2=\begin{cases}\frac{\lambda^S+2\mu^S+\rho_0^F\kappa+2Q}{\rho_0^S+\rho_0^F}\equiv\frac{1}{1+r}\left(c_{P1}^2+rc_{P2}^2+\frac{2Q}{\rho_0^S}\right) & \text{for P1}-\text{wave},\\ 0\quad\text{for P2}-\text{wave},\end{cases},$$
$$\lim_{\omega\to 0}k_I=0,\quad k_R\equiv\operatorname{Re}(k),\quad k_I\equiv\operatorname{Im}(k), \tag{44}$$

– high frequency limit $\omega\to\infty$

$$\lim_{\omega\to\infty}\left(\frac{\omega}{k_R}\right)^2=\begin{cases}c_1\equiv c_{P1}^2+\frac{1}{2}\left(c_{P1}^2-c_{P2}^2\right)(s-1) & \text{for P1}-\text{wave}\\ c_2\equiv c_{P2}^2-\frac{1}{2}\left(c_{P1}^2-c_{P2}^2\right)(s-1) & \text{for P2}-\text{wave}\end{cases}, \tag{45}$$

where the coupling parameter s is defined as follows

$$s := \sqrt{1 + \frac{4Q^2}{r\rho_0^{S2}\left(c_{P1}^2 - c_{P2}^2\right)^2}}, \tag{46}$$

and

$$\lim_{\omega\to\infty} k_I = \begin{cases} \frac{\pi}{2\rho_0^S c_1 s}\left[\frac{1}{2}(1+\frac{1}{r})(s-1) + 1 - \frac{\sqrt{s^2-1}}{\sqrt{r}}\right] & \text{for P1} - \text{wave} \\ \frac{\pi}{2\rho_0^S c_2 s}\left[\frac{1}{2}(1+\frac{1}{r})(s-1) + \frac{1}{r} + \frac{\sqrt{s^2-1}}{\sqrt{r}}\right] & \text{for P2} - \text{wave} \end{cases}. \tag{47}$$

It can be easily seen that the attenuation of P1-waves must be weaker for Biot's model ($s \neq 1$) than for the simple mixture model ($s = 1$). It is the other way around for P2-waves.

We obtain results for the simple mixture model by substituting $Q = 0$, i.e. $s = 1$. Clearly, this model is always stable (i.e. $k_I > 0$). The general dispersion relation in the case of this model simplifies as follows

$$k^4\left[\lambda^S + 2\mu^S\right]\rho_0^F\kappa - k^2\left\{\left(\rho_0^S\omega^2 + i\pi\omega\right)\rho_0^F\kappa + \left(\rho_0^F\omega^2 + i\pi\omega\right)\left[\lambda^S + 2\mu^S\right]\right\} +$$
$$+\left(\rho_0^S\omega^2 + i\pi\omega\right)\left(\rho_0^F\omega^2 + i\pi\omega\right) + \pi^2\omega^2 = 0. \tag{48}$$

This relation has been intensively investigated (e.g. [15, 16] where further references can be found). It has been shown that most of the qualitative features of solutions check well with this predicted by Biot's model [17].

We proceed to present numerical examples for all four models discussed above.

We use again the numerical data (30) and present results for the single Poisson's ratio $\nu = 0.2$ and two values of the initial porosity $n_0 = 0.24$ and 0.4. This choice leads to acceptable results for simplified models, more or less reasonable results for Biot's model and nonphysical results for the full model. Both points lie in the unstable region of the full model.

Let us begin with the P1-wave. This wave as well as the S-wave are commonly described in geotechnics by a single component model. The most important feature of these two modes are different limits for velocities of propagation for $\omega \to 0$ – the low frequency behavior, and for $\omega \to \infty$ – high frequency behavior. These two limits are different primarily due to the influence of the denominator in the relation for the velocity in which the first limit contains the full mass density of both components $\left(\rho_0^S + \rho_0^F\right) \equiv \rho_0^S(1+r)$, while for the second limit – solely the mass density of the skeleton ρ_0^S (see: relations (44) and (45)). This behavior is clearly seen in Figure 3 for both simplified models. Neither Biot's model nor the full model possess this property for P1-velocities. It is clearly due to the interactions described by material parameters Q and N because, firstly, S-waves do possess this property for all models and these waves are only very weakly influenced by couplings and, secondly, models without couplings ($Q = 0, N = 0$) possess this property as well. The P1-velocity in Biot's model remains constant practically in the whole range of frequencies, and the

P1-velocity in the full model is even slightly decaying. This is a rather disastrous consequence of Gassmann relations which apparently predict too high values of coupling coefficients Q, N – at least for the chosen points on the (ν, n_0)-plane.

Differences in the magnitude of P1-, and S-velocities are of the order of 20% but, if we accounted for the above fault of Biot's model and of the full model and reduced correspondingly the coupling coefficients to more realistic values, these differences would be much smaller.

The qualitative behavior of P2-velocities is the same for all models but the quantitative differences are even bigger than these for P1-velocities. Again, these results are not very relevant for practical applications because the coupling coefficients must be first corrected and this would increase P2-velocities obtained within Biot's model and the full model.

We proceed to discuss the attenuation of monochromatic waves shown in Figure 4. It is seen on the first glance that results for the attenuation of P1-waves practically disqualify both Biot's model and the full model. For Biot's model the attenuation lies still in the positive range but it is much too small from the physical point of view. This follows from the domination of the coupling, whose values were calculated according to classical Gassmann relations over the dissipation predicted by the permeability.

For the full model the attenuation is negative for both choices of parameters and, consequently, the model is unstable.

Attenuation of S-waves is almost not influenced by the coupling while the attenuation of P2-waves is much larger for models with couplings than for these without couplings. All of them are positive.

6 Conclusions

The above analysis shows that the qualitative behavior of models depends substantially on the application of Gassmann relations for a dependence of material parameters on the initial porosity n_0. We conclude that, in general, coupling coefficients Q, N, predicted by these relations are much too big. This yields a wrong behavior of low and high frequency limits of velocities of P1-waves within Biot's model as well as the full model. In addition, it leads to the independence of the velocity of P1-waves from the frequency in Biot's model and to the instability of the full model for parameters (ν, n_0) lying approximately below the line $\nu = n_0$. This instability does not seem to have any physical significance.

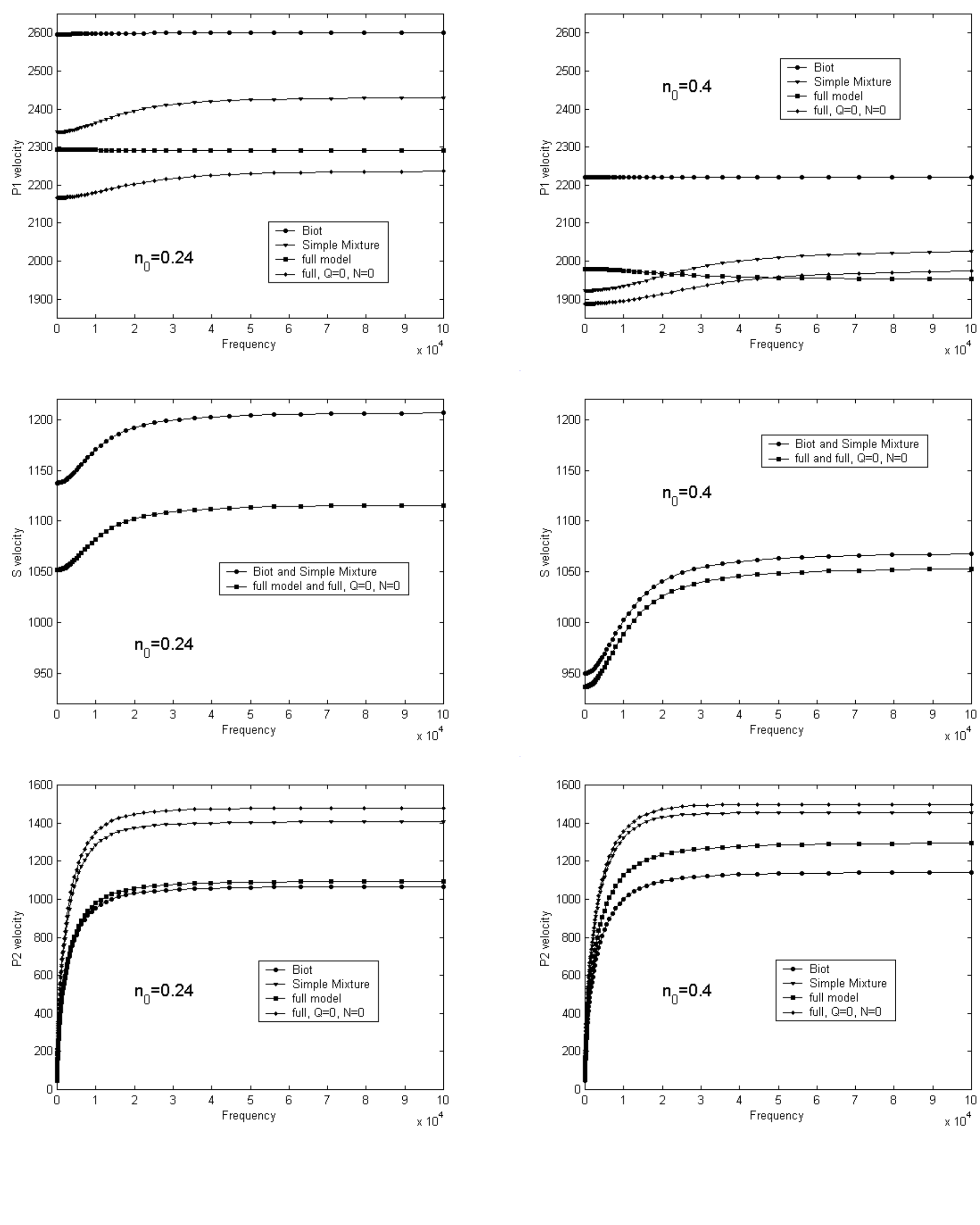

Figure 3: *Phase velocities for Poisson's ratio $\nu = 0.2$ and porosities $n_0 = 0.24$* and 0.4.

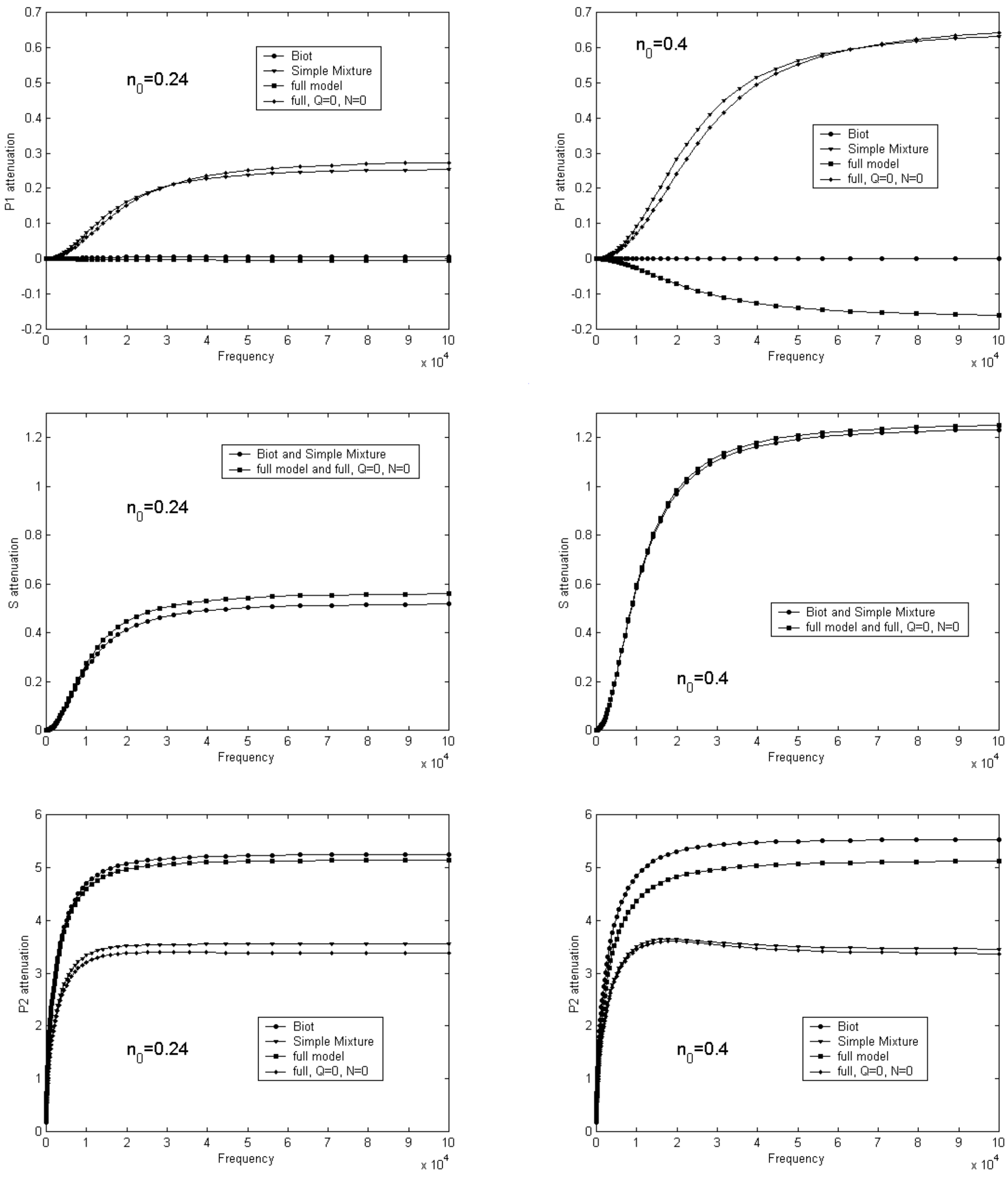

Figure 4: *Attenuation of monochromatic waves for Poisson's ratio* $\nu = 0.2$ *and porosities* $n_0 = 0.24$ and 0.4.

Apart from the above flaws all models behave in the similar way. They predict the same modes of propagation of bulk waves: P1-, P2-, and S-waves. They also predict the decay of the velocity of P2-wave with the frequency going to zero and this is the most important property of the second sound. In addition they all predict a much stronger attenuation of P2-waves than P1-waves.

If we limit the attention to Biot's model and its simplification with $Q = 0$ – the simple mixture model then we see that not only the qualitative behavior but also quantitative results for both models are quite similar. For the low frequency approximation the simpler model seems to be even better than Biot's model. This conclusion is important for the linear wave analysis in saturated poroelastic materials. In particular, the analysis of surface waves for the simple mixture model becomes much simpler than for Biot's model (e.g. [18]).

7 Appendix

In this Appendix we derive the relation (18) for the shear modulus μ^S. It is based on the assumption that the poroelastic material reacts on the external loading in the same way as the classical one-component elastic material under the condition of full draining, i.e.

$$\mathbf{T}^F - \mathbf{T}_0^F = 0. \tag{49}$$

Then, according to relations (10) we have

$$\varepsilon = -\frac{Q + N(n_0\delta + \Phi)}{\rho_0^F\kappa - N\Phi} e. \tag{50}$$

Consequently, for the full bulk stress we have

$$\begin{aligned}\mathbf{T} - \mathbf{T}_0 &:= \left(\mathbf{T}^S - \mathbf{T}_0^S\right) + \left(\mathbf{T}^F - \mathbf{T}_0^F\right) \equiv \mathbf{T}^S - \mathbf{T}_0^S = \\ &= \left\{\lambda^S - N(n_0\delta + \Phi) - (Q + \Phi N)\frac{Q + N(n_0\delta + \Phi)}{\rho_0^F\kappa - N\Phi}\right\} e\mathbf{1} + 2\mu^S\mathbf{e}^S.\end{aligned} \tag{51}$$

This relation is identical with Hooke's law of a one-component elastic material if

$$\begin{aligned}\lambda &= \lambda^S - N(n_0\delta + \Phi) - (Q + \Phi N)\frac{Q + N(n_0\delta + \Phi)}{\rho_0^F\kappa - N\Phi}, \\ \mu &= \mu^S,\end{aligned} \tag{52}$$

where λ, μ are Lamé constants of the one-component material.

If we use $\{\lambda, \nu\}$-parameters, where ν is the Poisson's ratio then it follows

$$\begin{aligned}\mu^S &= \frac{1-2\nu}{2\nu}\left\{\lambda^S - N(n_0\delta + \Phi) - (Q + \Phi N)\frac{Q + N(n_0\delta + \Phi)}{\rho_0^F\kappa - N\Phi}\right\} = \\ &= \frac{3}{2}\frac{1-2\nu}{1+\nu}\left\{K - \rho_0^F\kappa - 2Q - N(n_0\delta + \Phi) - (Q + \Phi N)\frac{Q + N(n_0\delta + \Phi)}{\rho_0^F\kappa - N\Phi}\right\},\end{aligned} \tag{53}$$

where (7) has been applied. Simultaneously, according to condition $(13)_3$ we have

$$K = K_d + \left(Q + \rho_0^F \kappa\right) \frac{Q + \rho_0^F \kappa - n_0 N}{\rho_0^F \kappa - n_0 N}. \tag{54}$$

Combination of these two relations yields

$$\mu^S = \frac{3}{2}\frac{1-2\nu}{1+\nu}\left\{K_d + Q\frac{Q+n_0 N}{\rho_0^F \kappa - n_0 N} - \frac{Q^2 + N\left[\rho_0^F \kappa \left(n_0 \delta + \Phi\right) + Q\left(n_0 \delta + 2\Phi\right)\right]}{\rho_0^F \kappa - \Phi N}\right\}, \tag{55}$$

which is the relation (18).

References

[1] L. Tisza; Transport phenomena in He II, *Nature*, 141, 1938.

[2] L. D. Landau; The theory of superfluidity of helium II, *J. Phys.* (U.S.S.R.). 5, 1941.

[3] I. Müller; *Thermodynamics*, Pitman, Boston, 1985.

[4] W. Dreyer, H. Struchtrup; Heat pulse experiments revisited, *Continuum Mech. Thermodyn.*, 5, 3-50, 1993.

[5] Ya. Frenkel; On the Theory of Seismic and Seismoelectric Phenomena in Moist Soil, *J. Phys.*, **8**, 230-241, 1944.

[6] Tolstoy, I.; *Acoustics, Elasticity, and Thermodynamics of Porous Media: Twenty-one Papers by M. A. Biot*, Acoustical Society of America, 1991.

[7] M. A. Biot; Theory of Propagation of Elastic Waves in a Fluid-Saturated Porous Solid. I. Low-Frequency Range, *Jour. Acoust. Soc. Am.,* **28**, 168-178, 1956. II. Higher Frequency Range, *Jour. Acoust. Soc. Am.*, **28**, 179-191, 1956.

[8] T. J. Plona; Observation of a Second Bulk Compressional Wave in a Porous Medium at Ultrasonic Frequencies: *Appl. Phys. Lett.*, **36**, 259–261, 1980.

[9] T. Klimentos, C. McCann; Why is the Biot Slow Compressional Wave not Observed in Real Rocks? *Geophysics*, **53**, 12, 1605–1609, 1988.

[10] K. Wilmanski; Thermodynamical Admissibility of Biot's Model of Poroelastic Saturated Materials, *Arch. Mech.*, **54**, 5-6, 709-736, 2002.

[11] K. Wilmanski; *Thermomechanics of Continua*, Springer, Heidelberg, Berlin, N.Y., 1998.

[12] R. D. Stoll; *Sediment Acoustics*, Lecture Notes in Earth Sciences, #26, Springer-Verlag, New York, 1989.

[13] J. E. White; *Underground Sound. Application of Seismic Waves*, Elsevier, Amsterdam, 1983.

[14] K. Wilmanski; On a Micro-macro Transition for Poroelastic Biot's model and Corresponding Gassmann-Type Relations, WIAS-Preprint #868, 2003; see also: *Geotechnique* (submitted for publication).

[15] K. Wilmanski; Waves in Porous and Granular Materials, in: *Kinetic and Continuum Theories of Granular and Porous Media*, CISM, Courses and Lectures #400, K. HUTTER, K. WLMANSKI (eds.), 131 - 185, Springer, Wien, N.Y., 1999.

[16] K. Wilmanski, B. Albers; Acoustic Waves in Porous Solid-Fluid Mixtures, in: *Dynamic Response of Granular and Porous Materials under Large and Catastrophic Deformations*, K. HUTTER, N. KIRCHNER (eds.), Lecture Notes in Applied and Computational Mechanics, Vol. 11, Springer, Berlin, 285-314, 2002.

[17] T. Bourbie, O. Coussy, B. Zinszner; *Acoustics of Porous Media*, Editions Technip, Paris, 1987.

[18] B. Albers; Surface Waves in Two-Component Poroelastic Media on Impermeable Boundaries - Numerical Analysis in the Whole Frequency Domain, WIAS-Preprint #862, 2003.